Dynamic Molecular Processes Detected by Microtubular Opto-chemical Sensors Self-Assembled from Prestrained Nanomembranes

Libo Ma, Shilong Li, Vladimir A. Bolaños Quiñones, Lichun Yang, Wang Xi, Matthew Jorgensen, Stefan Baunack, Yongfeng Mei, Suwit Kiravittaya, and Oliver G. Schmidt*

Rolled-up nanotech[1,2] has opened up broad interdisciplinary research in areas ranging from nanophotonics, nanoelectronics and magnetoelectronics to nanorobotics, biophysics and catalytic chemistry. For example, functional units based on rolled-up nanomembranes include optical ring resonators,[3,4] ultra-compact energy storage devices,[5,6] magnetic sensors,[7] spin-wave resonators,[8] novel concepts for metamaterials[9,10] and superconducting devices[11] as well as autonomous microengines[12,13] and full lab-in-a-tube systems.[14,15] The possibility to shape nanomembranes out of many different materials and material combinations into vertical optical ring resonators[3,4] is particular exciting and has led to the fabrication of microtube lasers[16,17] and optofluidic components,[18–20] which are extremely sensitive to refractive index changes caused by different fluids inserted into the hollow core of the microtube.[19,20] Because the light is guided by and within the sub-wavelength thin walls of the rolled-up microtube, the evanescent part of the confined whispering gallery modes (WGM) is expected to be particularly sensitive to tiny alterations and modifications in the vicinity of the inner and outer tube wall surfaces.

Optical WGMs have been used previously as a surface sensitive technique because of their label-free ability to obtain quantitative information about molecular bindings on the surface in real time. Recently, single bio-molecule/particle detection has been demonstrated with ultra-high-Q microtoroidal and microspherical systems.[21–23] The detection of protein membranes on a microsphere surface as well as gas molecule condensation on an AlGaAs microdisk surface at low temperature has also been explored.[24,25] Here, we employ nanomembrane based optical ring resonators for sensitive surface detection in real time under ambient conditions, which allows us to collect detailed information about surface molecular dynamic processes of submonolayer thick H_2O and C_2H_5OH. The interaction of H_2O molecules with solid surfaces has attracted much attention, affecting various research fields ranging from atmospheric chemistry[26] to corrosion[27] and heterogeneous catalysis.[28] Since rolled-up microtubes naturally assume a hollow channel/pipeline[29] and are fully integratable into lab-on-chip systems,[20] a practical opto-chemical gas sensor with outstanding properties is possible in the near future.

In this work, asymmetric microtube cavities were fabricated for dynamic molecular process detection. The microcavities were prepared by releasing and curling differentially strained SiO/SiO_2 bilayer nanomembranes into microtube structures on a silicon substrate. These kind of tubes provide an enhanced Q-factor that favors highly sensitive detection.[30] Measurements were performed near the opening of these tubes where the wall has less than two windings (i.e. part of the tube wall consists of a single-layered nanomembrane). The tube diameter measures around 5.8 μm, which is close to the minimum achievable size for low refractive index micro-resonators working in the visible spectral range. After the roll-up process, a 30 nm thick film of hafnium oxide (HfO_2) was grown on the microtube surface using atomic-layer-deposition (ALD) to increase the structural stability.[31] Dynamic molecular processes of H_2O and C_2H_5OH are detected on the thin nanomembrane surface. Through the detection of molecular interactions, a robust ice-like H_2O molecule layer on the microtube surface was revealed. Based on perturbation theory, quantitative information of molecule layer changes on the tube surface was acquired.

Figure 1a shows a schematic diagram of a microtube rolled-up from a SiO/SiO_2 bilayer nanomembrane and coated with HfO_2 by ALD. The microtube surface is terminated by Hf–O bonds which are more polar than Si–O bonds in SiO_x.[32] A cross-sectional scanning electron microscopy (SEM) image of a representative rolled-up microtube (applying a technique developed by Deneke et al.[33]) with a diameter of around 8 μm is shown in Figure 1b. Due to a much higher dielectric constant ($\varepsilon \approx 25$) than that of silicon oxide ($\varepsilon \approx 3.9$), the ALD coated HfO_2

Dr. L. B. Ma, S. L. Li, V. A. Bolaños Quiñones, Dr. L. C. Yang, Dr. W. Xi, Dr. M. Jorgensen, Dr. S. Baunack, Prof. Dr. O. G. Schmidt
Institute for Integrative Nanosciences
IFW Dresden, Helmholtzstrasse 20,
Dresden D-01069, Germany
E-mail: lbmacn@gmail.com
Prof. Y. F. Mei
Department of Materials Science
Fudan University
Shanghai 200433, China
Dr. S. Kiravittaya
Department of Electrical and Computer Engineering
Naresuan University
Phitsanulok 65000, Thailand
Prof. O. G. Schmidt
Material Systems for Nanoelectronics
Chemnitz University of Technology
Reichenhainer Str. 70, Chemnitz D-09107, Germany

DOI: 10.1002/adma.201204065

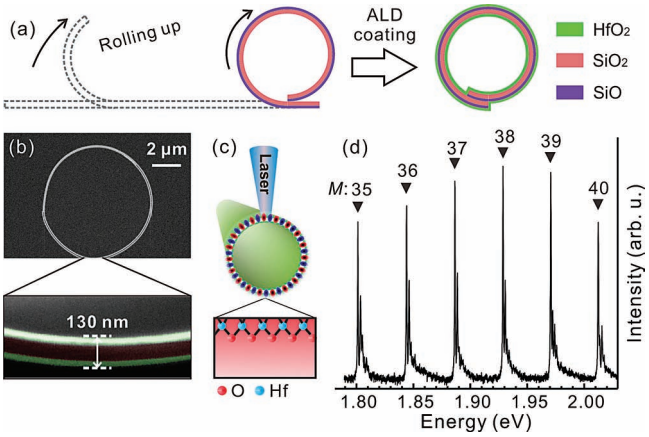

Figure 1. Schematic diagram of: a) a microtube that is self-assembled by rolling-up from a SiO/SiO_2 bilayer nanomembrane and coated with HfO_2 by ALD deposition. b) Cross-section SEM image of a rolled-up microcavity reveals a layered tube wall structure (see bottom panel), where the HfO_2 layers show bright traces, while the middle SiO/SiO_2 bilayers (two SiO/SiO_2 bilayers here) show a dark trace. c) Sketch of optical resonant mode profile in the cross section of a microtube cavity excited by a laser beam. The evanescent field extends beyond the Hf–O bonds terminating the tube surface. d) High-Q resonant mode spectrum labeled with azimuthal mode numbers $M = 35$ to 40.

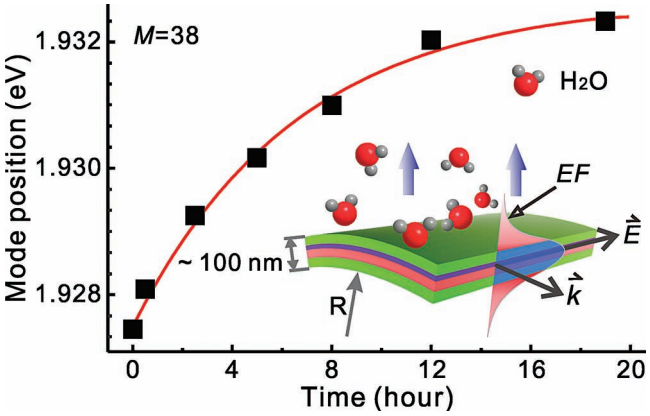

Figure 2. Dynamic desorption process of H_2O molecules from the microtube surface recorded by monitoring mode ($M = 38$) position as a function of drying time in a desiccator. The process is fitted by the LDF model (red curve). The resonant light, shown in the inset, propagates ($\vec{k}$ direction) in a ≈100 nm-thick tube wall and the evanescent field (*EF*) greatly extends out of the tube surface.

layer appears in high-contrast (white trace in the wall layers) while the SiO/SiO_2 bilayer structures in the middle are difficult to discriminate under electron beam scanning. The high polarity of Hf–O bonds[32,34] on the tube surface leads to a pronounced affinity for polar molecular adsorption. Figure 1c shows a sketch of a laser beam exciting the microtube at a specific lateral position and the generated optical mode profile in the ring-shaped cross section. Due to the special asymmetric tube geometry, the resonant light is confined laterally to a region approximately 3 μm wide near the open end of the tube.[30] Figure 1d shows the resonant mode spectrum revealing distinct high-Q resonant modes which are labelled with calculated azimuthal mode numbers *M*. The *Q* factor is ≈2000 which is in the range of the highest reported for a rolled-up microtube composed of *low* refractive index materials.[20] Due to the subwavelength thick tube wall, the evanescent field substantially leaks out of the tube surface, greatly enhancing the surface detection sensitivity. When the surface environment slightly changes, the evanescent field is perturbed and the resonant modes either red- or blue-shift. Since all the modes shift concurrently in response to the surface changes, only one of the modes is needed for the sensing measurement of the molecular adsorption/desorption kinetics. The mode corresponding to $M = 38$ was selected for the measurements discussed here.

Figure 2 shows the detection of the dynamic desorption process of H_2O molecules from the HfO_2 terminated nanomembrane surface. As an inverse process of molecular adsorption, the desorption can be described based on the linear-driving-force (LDF) model which was originally developed for molecular absorption.[35] In ambient environment, the H_2O molecules in air are readily adsorbed onto the HfO_2 surface to form a natural wetting layer. It should be noted that the tube surface was sufficiently dried and kept clean before exposure to air. When the adsorption and desorption rates of H_2O molecules are balanced on the HfO_2 surface, the H_2O layer reaches a dynamic equilibrium with a stable thickness. After wetting at ambient conditions, the microtube cavity was then transferred into a drying chamber to remove the adsorbed H_2O molecules from the tube surface. In this new environment, the equilibrium of the surface dynamic process is broken and the H_2O molecules start to migrate away from the HfO_2 surface. As shown in Figure 2, the mode position continuously blueshifts with drying time representing the continuous desorption process of H_2O molecules. Over time (>19 hours), the mode position approaches a constant value indicating that the tube has almost completely dried. Based on our numerical calculations (shown below), quantitative information about the molecular layer can be obtained. In this experiment, the total mode shift is $\Delta E \approx 4.87$ meV, which is equivalent to a change of H_2O layer thickness of $\Delta h \approx 2.0$ nm (≈8 monolayers).

Our optical microcavity was also applied to the dynamic detection of ethanol adsorption/desorption on the nanomembrane surface. For this study, a droplet of ethanol was applied to the tube surface which has been completely dried beforehand. The ethanol droplet rapidly spread across the tube surface and quickly dries within a few seconds. In this way an out-of-equilibrium C_2H_5OH layer was generated on the HfO_2. After the C_2H_5OH layer has been generated, the mode redshifts by $\Delta E \approx 3.47$ meV with respect to the initial case of the dried surface, which implies an adsorption thickness of a $\Delta h \approx 1.36$ nm (≈2.9 monolayer) C_2H_5OH layer on the HfO_2 tube surface. As shown in **Figure 3**, the mode position of the C_2H_5OH layer coated tube cavity quickly blueshifts when the tube surface was exposed to air. The experimental data are fitted by the LDF model taking into account the bidirectional dynamic process of desorption of C_2H_5OH and adsorption of H_2O molecules. During the initial stage, the mode energy continuously blueshifts reflecting the desorption process of the C_2H_5OH molecules which is much faster than that of H_2O as shown in Figure 3. The mode energy blueshift of $\Delta E \approx 1.12$ meV translates

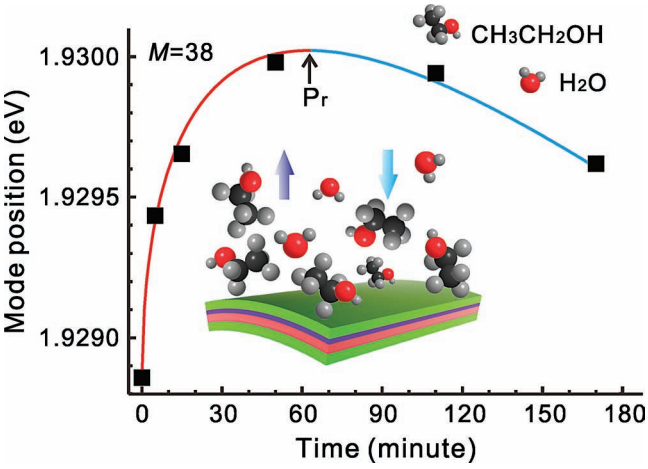

Figure 3. Bidirectional dynamic process of desorption of C_2H_5OH and adsorption of H_2O are detected on tube surface. A turning point (P_r) is revealed at around 60- min, where the inversion between the desorption and adsorption process occurs. The whole process is fitted by the LDF model taking into account the bidirectional dynamic process.

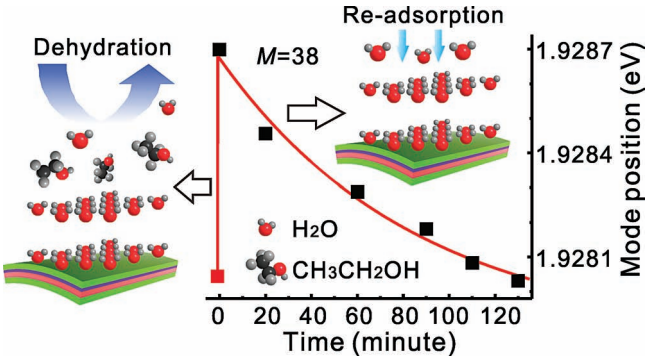

Figure 4. Mode (M = 38) blue-shift of ΔE = 0.66 meV implying desorption of around one H_2O monolayer after ethanol dehydration on the tube surface. The subsequent red-shift of the mode position indicates a re-adsorption process of the H_2O molecules, which is fitted by the LDF model.

into a thickness change of $\Delta h \approx 0.48$ nm for the C_2H_5OH desorbed layer, which is around one C_2H_5OH monolayer. The H_2O molecule has a much stronger hydrogen bonding strength than C_2H_5OH. Hence, once the C_2H_5OH molecules are desorbed from the surface, the vacancies are immediately occupied by H_2O molecules from air. The surface evolution therefore consists of a subtle bidirectional dynamic process combining desorption of C_2H_5OH and adsorption of H_2O molecules. The bidirectional process reaches a transient equilibrium at around 60 min marking a turning point (P_r) where an inversion between desorption of C_2H_5OH and adsorption of H_2O occurs. In the first 60 minutes, the desorption of C_2H_5OH dominates the surface molecule layer change and therefore leads to a continuous blueshift of the mode. After longer exposure time in air, H_2O molecule adsorption takes over and, as a result, the mode energy starts to redshift. This result implies that the microtube cavity, as a smart opto-chemical detector, is well-suited to sense and track non-equilibrium dynamics of molecular adsorption/desorption on a solid surface.

It is well known that strong hydrogen bonding is formed between C_2H_5OH and H_2O. When the two molecules are close they attract each other and the H_2O molecule is easily carried away by the more volatile C_2H_5OH. **Figure 4** shows the detection of the dehydration effect on the nanomembrane surface. The previously dried HfO_2 surface was wetted by room atmosphere moisture as discussed before. Afterwards, a droplet of C_2H_5OH was dispensed onto the HfO_2 surface and the C_2H_5OH dries quickly. The resonant mode positions were recorded before and after dispensing the ethanol on the surface. Compared to the dried case in Figure 2, there is a $\Delta E \approx$ 4.27 meV difference of mode positions in the naturally wetted nanomembrane (i.e., ≈7.3 monolayers of H_2O were initially adsorbed on the tube surface). After the ethanol was dispensed, the mode jumps to a higher energy by ΔE = 0.66 meV, corresponding to $\Delta h \approx 0.28$ nm (i.e., ≈1 monolayer change in H_2O). Supposing that the 7.3 monolayers H_2O were totally removed and substituted by an ethanol layer, the mode position should blueshift as shown in Figure 3. In contrast, the mode position immediately redshifts implying a re-adsorption of H_2O molecules. This result indicates that only around one monolayer of H_2O was removed from the total ≈7.3 monolayers on the HfO_2 tube surface. The suppression of the ethanol dehydration effect suggests that the H_2O molecules assemble into a durable ice-like layer on the surface, as has been discussed previously both theoretically and experimentally.[36–38] In contrast to previous reports, here the robust ice-like H_2O molecule structure was detected at room temperature on a nanomembrane platform assisted by optical resonances. The robust H_2O film thickness of ≈7 monolayers detected here on the HfO_2 surface is thicker than what was observed on mica substrates,[37] and is in the range theoretically predicted for H_2O on quartz substrates.[38] It should be noted that this robust H_2O layer can be removed if exposed to a dry atmosphere for a long time. This observation is interesting for the studies of dehydration on solid surfaces wetted with molecular layers of water or bioadhesion on solid surfaces.[39]

Since the molecular layer thickness is much smaller than the tube diameter, perturbation theory is a suitable tool to calculate the mode shift induced by small structural changes on the cavity surface.[31,40] Based on this method, the thin molecule layer induced mode shift ($\Delta\omega$) is calculated by:

$$\Delta\omega = -\frac{\omega}{2}\frac{\langle E(\vec{r})|\Delta\varepsilon(\vec{r})|E(\vec{r})\rangle}{\langle E(\vec{r})|\varepsilon(\vec{r})|E(\vec{r})\rangle} \quad (1)$$

where $\varepsilon(\vec{r})$, ω and $E(\vec{r})$ are the permittivity, resonance angular frequency, and the electric field distribution in the ring resonator model, respectively. $\Delta\varepsilon(\vec{r})$ is the variation of permittivity induced by the molecule layer. A refractive index of 1.333 for the water molecule layer and 1.359 for the ethanol molecule layer were used for calculations. Here the bulk refractive indices of water and ethanol were used to analyze the molecular layer changes on the tube surface, since there is still a huge amount of molecules (>10^8) on the tube surface per monolayer. For the single or few molecules case, one should consider molecular rather than macroscopic refractivity to more precisely calculate the mode changes. In the calculation, the molecular layers on both the inner and outer tube surface are

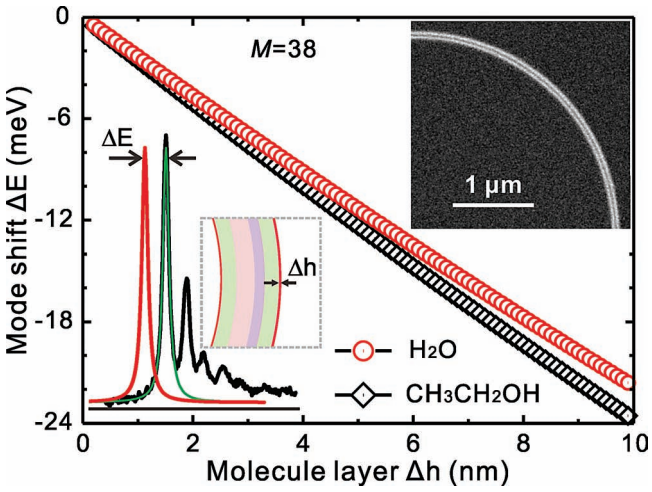

Figure 5. Optical resonant mode ($M = 38$) shift (ΔE) induced by adsorbed molecule layer (Δh) on both outer and inner tube surfaces calculated using perturbation theory for H_2O and C_2H_5OH molecules, respectively. The upper right inset shows the cross-section SEM image of the part tube wall rolled-up from nanomembrane. The bottom left inset shows the schematic of resonant mode shift in response to adsorbed molecular layer on the nanomembrane surfaces.

considered. **Figure 5** shows the calculated mode shift (ΔE) as a function of the adsorbed molecular layer thickness (Δh). As expected, the higher refractive index molecule layer will lead to a larger mode shift. Taking into account the Q-factor and the sensitivity[41] to molecule adsorbance, in principle a minimum mode shift of $\Delta E \approx 0.02$ meV (i.e. effective partial coverage of 0.034 for H_2O and 0.017 for C_2H_5OH could be detected on the nanomembrane formed microtube surface).

The broad interest in this work rests on the fact that surface phenomena can be detected in real time by optical resonances in microtube cavities self-assembled from nanomembranes. The tube surfaces can be flexibly ALD coated by various other materials (e.g., Al_2O_3, TiO_2). Such materials provide alternative properties which are beneficial for specific surface chemical reactions, especially for photochemical reactions, or surface catalysis, etc. With functionalization, the optical microtube cavity may also be a useful tool to detect pollution traces by selectively binding specific molecules like CO, NO_2, and SO_2, to the tube surface. Moreover, one can use bio-functionalized surfaces of the tube cavity[15,42] for selective sensing of biomolecules such as proteins and DNA fragments. In addition, this work also opens a path to optically detect subtle surface modifications like surface reconstructions, or adsorbate-induced reconstructions. Those studies would pave the way for surface science explored by optical resonances in nanomembrane assembled microsystems.

In conclusion, we have demonstrated that dynamic molecular processes can be detected by optical resonances in nanomembrane formed microtube cavities. The microtube cavities are prepared by rolling-up prestrained nanomembranes on a silicon substrate which are subsequently covering by a thin HfO_2 film using ALD. The microtube cavity in which optical resonances are excited around its perimeter represents an elegantly conceived whispering-gallery-mode sensor for detection of molecular kinetics. Based on perturbation theory, quantitative information of molecule layer changes on the tube surface is acquired. The combination of optical resonances with nanomembrane surfaces opens up a promising platform to detect surface phenomena with optical methods. Due to the sub-wavelength tube wall and relatively small tube diameter, the evanescent field considerably penetrates out of the tube surface allowing for a highly sensitive response to surface molecular changes. The desorption process of naturally adsorbed H_2O molecule layers is detected by drying the tube surface. A faster desorption process of C_2H_5OH molecules from the HfO_2 surface is observed due to its smaller polarity compared to H_2O molecules. A dynamic bidirectional process of desorption of C_2H_5OH and adsorption of H_2O molecules was observed. A robust ice-like H_2O molecular layer on the nanomembrane based microtube cavity was revealed through detecting molecular interactions at room temperature. The ability of our microtube cavity to probe molecular level changes on the sensing surface constitutes a versatile platform for the detection of diverse surface phenomena in a label-free fashion.

Experimental Section

Microtube Cavity Fabrication and HfO_2 Surface Coating: The rolled-up optical resonators were prepared by releasing and curling a differentially strained SiO/SiO_2 bilayer nanomembranes into microtube structures on a silicon substrate.[43] In contrast to previous reports, the microtube resonators used in this work were prepared by releasing a SiO/SiO_2 bilayer from a sloped photoresist pattern. The sloped photoresist layer was prepared by taking advantage of centrifugal force discrepancy using an off-center spin coating technique. Afterwards, a 6 nm SiO layer and a 27 nm SiO_2 layer were deposited on the photoresist patterns, at different rates to induce strain. By dissolving the photoresist in acetone, the free-standing nanomembranes released their strain by rolling into tubular structures in a slightly tilted fashion resulting in asymmetric cone-like microtubes with a gradual diameter variation along their axis.[30] This kind of tube provides an enhanced Q-factor which opens a way for highly sensitive detection. After the roll-up process, a 30 nm thick film of hafnium oxide (HfO_2) was grown on the microtube surface using atomic-layer-deposition (ALD) to increase the structural stability.

Optical Characterization: Optical resonant mode spectra of the microtube cavity were measured at room temperature by a conventional micro-photoluminescence (μ-PL) setup equipped with a He-Cd laser line at 442 nm (50 μW) for excitation. The laser optically excites nonbridging oxygen hole center (≡Si–O·) defects[44] in the amorphous silicon oxide nanomembrane which serve as light emitters in the visible spectral range. Optical resonant modes were formed by constructive interference of light circulating in the tube wall. The excitation laser was focused through a 50× microscope objective and the emission signal was collected through the same objective to record the spectra.

Molecule Layer Loading/Release On/From the Tube Surface: The high electronegativity difference in the Hf–O system on the tube surface leads to a higher affinity for polar water molecule adsorption. Under atmospheric condition, the H_2O molecules in air are readily adsorbed onto polar HfO_2 surfaces to form a natural wetting layer on the tube surface. By putting the naturally wetted microtube into a desiccator, desorption of H_2O molecules is observed due to the dynamic equilibrium broken on the surface H_2O layer. The resonant mode spectra are measured in turn according to the drying time in the desiccator. For the ethanol molecule desorption study, a droplet of ethanol was dispensed onto a dried tube surface using a microfluidic syringe pump. The ethanol droplet immediately wet the tube surface and rapidly dried within a few seconds, leaving an adsorbed ethanol layer on the tube

surface. For the ethanol dehydration detection, a droplet of ethanol was applied to a sufficiently wetted tube surface under ambient environment. The resonant mode spectrum was immediately measured after the ethanol droplet was applied.

Supporting Information

Supporting Information is available from the Wiley Online Library or from the author.

Acknowledgements

This work was supported by the Volkswagen Foundation (I/84072), the U.S. Air Force Office of Scientific Research MURI program under Grant FA9550-09-1-0550, and the DFG priority program FOR 1713. S.L.L. thanks the financial support from China Scholarship Council (CSC, File No. 2008617109). L.B.M. thanks the support from National Science Foundation of China (NSFC) with the Grant No. 11104343.

Received: September 27, 2012
Revised: January 4, 2013
Published online: March 1, 2013

[1] V. Y. Prinz, V. A. Seleznev, A. K. Gutakovsky, A. V. Chehovskiy, V. V. Preobrazhenskii, M. A. Putyato, T. A. Gavrilova, *Physica E* **2000**, *6*, 828.
[2] O. G. Schmidt, K. Eberl, *Nature* **2001**, *410*, 168.
[3] T. Kipp, H. Welsch, C. Strelow, C. Heyn, D. Heitmann, *Phys. Rev. Lett.* **2006**, *96*, 077403.
[4] R. Songmuang, A. Rastelli, S. Mendach, O. G. Schmidt, *Appl. Phys. Lett.* **2007**, *90*, 091905.
[5] C. C. Bof Bufon, J. D. Cojal González, D. J. Thurmer, D. Grimm, M. Bauer, O. G. Schmidt, *Nano Lett.* **2010**, *10*, 2506.
[6] H. X. Ji, Y. F. Mei, O. G. Schmidt, *Chem. Commun.* **2010**, *46*, 3881.
[7] I. Mönch, D. Makarov, R. Koseva, L. Baraban, D. Karnaushenko, C. Kaiser, K.-F. Arndt, O. G. Schmidt, *ACS Nano* **2011**, *5*, 7436.
[8] F. Balhorn, S. Mansfeld, A. Krohn, J. Topp, W. Hansen, D. Heitmann, S. Mendach, *Phys. Rev. Lett.* **2010**, *104*, 037205.
[9] E. J. Smith, Z. Liu, Y. F. Mei, O. G. Schmidt, *Nano Lett.* **2010**, *10*, 1.
[10] S. Schwaiger, M. Bröll, A. Krohn, A. Stemmann, C. Heyn, Y. Stark, D. Stickler, D. Heitmann, S. Mendach, *Phys. Rev. Lett.* **2009**, *102*, 163903.
[11] V. M. Fomin, R. O. Rezaev, O. G. Schmidt, *Nano Lett.* **2012**, *12*, 1282.
[12] A. A. Solovev, Y. Mei, E. Bermúdez Ureña, G. Huang, O. G. Schmidt, *Small* **2009**, *5*, 1688.
[13] Y. F. Mei, A. A. Solovev, S. Sanchez, O. G. Schmidt, *Chem. Soc. Rev.* **2011**, *40*, 2109.
[14] E. J. Smith, S. Schulze, S. Kiravittaya, Y. Mei, S. Sanchez, O. G. Schmidt, *Nano Lett.* **2011**, *11*, 4037.
[15] E. J. Smith, W. Xi, D. Makarov, I. Monch, S. Harazim, V. A. Bolanos Quinones, C. K. Schmidt, Y. Mei, S. Sanchez, O. G. Schmidt, *Lab Chip* **2012**, *12*, 1917.
[16] F. Li, Z. T. Mi, *Opt. Express* **2009**, *17*, 19933.
[17] C. Strelow, M. Sauer, S. Fehringer, T. Korn, C. Schuller, A. Stemmann, C. Heyn, D. Heitmann, T. Kipp, *Appl. Phys. Lett.* **2009**, *95*, 221115.
[18] A. Bernardi, S. Kiravittaya, A. Rastelli, R. Songmuang, D. J. Thurmer, M. Benyoucef, O. G. Schmidt, *Appl. Phys. Lett.* **2008**, *93*, 094106.
[19] V. A. Bolaños Quiñones, L. B. Ma, S. L. Li, M. Jorgensen, S. Kiravittaya, O. G. Schmidt, *Appl. Phys. Lett.* **2012**, *101*, 151107.
[20] S. Böttner, S. L. Li, J. Trommer, S. Kiravittaya, O. G. Schmidt, *Opt. Lett.* **2012**, *37*, 5136.
[21] A. M. Armani, R. P. Kulkarni, S. E. Fraser, R. C. Flagan, K. J. Vahala, *Science* **2007**, *317*, 783.
[22] L. N. He, S. K. Ozdemir, J. Zhu, W. Kim, L. Yang, *Nat. Nanotechnol.* **2011**, *6*, 428.
[23] F. Vollmer, S. Arnold, D. Keng, *Proc. Natl. Acad. Sci. USA* **2008**, *105*, 20701.
[24] F. Vollmer, D. Braun, A. Libchaber, M. Khoshsima, I. Teraoka, S. Arnold, *Appl. Phys. Lett.* **2002**, *80*, 4057.
[25] K. Srinivasan, O. Painter, *Appl. Phys. Lett.* **2007**, *90*, 031114.
[26] B. J. Finlayson-Pitts, J. N. J. Pitts, *Atmospheric Chemistry: Fundamentals and Experimental Techniques*, Wiley, New York **1986**.
[27] C. Leygraf, *Encyclopedia of Electrochemistry*, Wiley-VCH, Weinheim, Germany **2007**.
[28] B. M. Reddy, P. Bharali, P. Saikia, A. Khan, S. Loridant, M. Muhler, W. Grünert, *J. Phys. Chem. C* **2007**, *111*, 1878.
[29] O. G. Schmidt, N. Y. Jin-Phillipp, *Appl. Phys. Lett.* **2001**, *78*, 3310.
[30] V. A. Bolaños Quiñones, L. B. Ma, S. L. Li, M. Jorgensen, S. Kiravittaya, O. G. Schmidt, *Opt. Lett.* **2012**, *37*, 4284.
[31] L. B. Ma, S. Kiravittaya, V. A. Bolaños Quiñones, S. L. Li, Y. F. Mei, O. G. Schmidt, *Opt. Lett.* **2011**, *36*, 3840.
[32] D. R. Lide, *CRC Handbook of Chemistry and Physics: A Ready-reference Book of Chemical and Physical Data*, CRC Press, Boca Raton, FL, USA **2004**.
[33] C. Deneke, U. Zschieschang, H. Klauk, O. G. Schmidt, *Appl. Phys. Lett.* **2006**, *89*, 263110.
[34] S. Takeda, M. Fukawa, Y. Hayashi, K. Matsumoto, *Thin Solid Films* **1999**, *339*, 220.
[35] C. R. Reid, K. M. Thomas, *Langmuir* **1999**, *15*, 3206.
[36] Q. Du, E. Freysz, Y. R. Shen, *Science* **1994**, *264*, 826.
[37] P. B. Miranda, L. Xu, Y. R. Shen, M. Salmeron, *Phys. Rev. Lett.* **1998**, *81*, 5876.
[38] J. Yang, S. Meng, L. F. Xu, E. G. Wang, *Phys. Rev. Lett.* **2004**, *92*, 146102.
[39] S. Margel, E. A. Vogler, L. Firment, T. Watt, S. Haynie, D. Y. Sogah, *J. Biomed. Mater. Res.* **1993**, *27*, 1463.
[40] S. G. Johnson, M. Ibanescu, M. A. Skorobogatiy, O. Weisberg, J. D. Joannopoulos, Y. Fink, *Phys. Rev. E* **2002**, *65*, 066611.
[41] H. Zhu, I. M. White, J. D. Suter, M. Zourob, X. Fan, *Anal. Chem.* **2006**, *79*, 930.
[42] S. Sanchez, A. A. Solovev, Y. Mei, O. G. Schmidt, *J. Am. Chem. Soc.* **2010**, *132*, 13144.
[43] Y. F. Mei, G. S. Huang, A. A. Solovev, E. Bermúdez Ureña, I. Mönch, F. Ding, T. Reindl, R. K. Y. Fu, P. K. Chu, O. G. Schmidt, *Adv. Mater.* **2008**, *20*, 4085.
[44] L. B. Ma, T. Schmidt, C. Jäger, F. Huisken, *Phys. Rev. B* **2010**, *82*, 165411.